Characterization of Dispersion-Hardened Electrodeposited Gold Composites. Part 1: SIMS and SEM Study of Powder Inclusions

S. Barison, S. Daolio, and M. Fabrizio*

IPELP CNR, Corso Stati Uniti 4, 35127 Padova, Italy

C. Piccirillo

High Vacuum Process srl, via R. Azzoni 3/b, 43100 Parma, Italy

I. Calliari

Department DIMEG, via Marzolo, 35131 Padova, Italy

L. Armelao

CSSRCC CNR Dept CIMA, via Marzolo 1, 35131 Padova, Italy

Received March 24, 2000. Revised Manuscript Received July 4, 2000

Submicrometric ceramic powders used as hardening agents for electrodeposited gold films were studied. Codeposits were obtained from a CN-free mixed electrolyte with or without the addition of a brightening agent. Secondary ion mass spectrometry (SIMS) and scanning electron microscopy (SEM) were applied to characterize the deposits. SIMS analysis gave useful information about the presence and distributions of additives in the films, and the influence of powders on metal-substrate interdiffusion phenomena were also shown. Surface morphology characteristics depending on experimental conditions, and the presence of additives were evidenced by SEM microscopy. Preliminary hardness tests were also carried out to evaluate the effectiveness of additives as hardening agents.

Introduction

Electroformed jewelry is obtained by electrodeposition of thick films (50−300 μm) of gold or its alloys on properly fashioned cathodes. When the desired thickness has been reached, the electrodeposition is stopped, and the conductive substrate is removed by acidic or thermal dissolution. In this way, the self-standing gold film maintains the same shape of the original cathode, and finally the object is achieved after thermal aging and mechanical polishing.

In comparison with rolling, the galvanic process gives objects with a high volume/weight ratio and fine detail definition, as well as the investment casting can provide. Cyanide complexes are the complexes most frequently used for electroforming, because of the high stability of the Au(I) complex and the bright appearance of deposits. The inclusive cost of these objects, however, is about 15% higher than those for molded ornaments because of the equipment investment and the additional charge for bath draining. Cyanide, in fact, is a very toxic compound and needs to be manipulated and drained carefully, as shown by the recent ecological disaster in Eastern Europe.

In the past few years, several cyanide-free alternative electrolytes have been developed,[1−7] but they are devoted mainly to microelectronics.[3,7] They exhibit good stability constants, suitable redox potential, and good throwing power; nevertheless, the use of these complexes is not common in jewelry electroforming production because their syntheses are laborious and the baths need stabilizers and/or brighteners to lengthen the electrolyte service life and promote suitable film growth.

As described elsewhere,[1] an electrolyte based on a sulfite−ethylenediaminetetracetate (EDTA) complex has been studied in this laboratory, and the obtained gold deposits were of a bright pure color, with good deposition rate and faradic efficiency.

However, as described in the literature,[8] high-fineness gold (mainly Au electrodeposited from these complexes) is a soft material, which needs hardening to improve its workability and resistance to wear. The hardening features of TiO_2, Al_2O_3, and SiC powders have been applied successfully to galvanic processes,[9−12] and SiC, B_4C, and TiN have also recently been used for gold electrodeposition[13,14] in CN-based baths. With the same aim, on the basis of some preliminary results,[1,15] this paper describes a study on the codeposition process of gold with electrochemically inert submicrometric ce-

(1) Fabrizio, M.; Piccirillo, C.; Daolio, S. *Rapid Commun. Mass Spectrom.* **1998**, *12*, 857.
(2) Trejo, G.; Gil, A. F.; Gonzàlez, J. *J. Appl. Electrochem.* **1996**, *26*, 1287.
(3) Honma, H.; Hagiwara, K. *J. Electrochem. Soc.* **1995**, *142*, 81.
(4) Morrissey, R. J. *Plat. Surf. Finish.* **1993**, *80*, 75.
(5) Sullivan, M.; Kohl, P. A. *J. Electrochem. Soc.* **1995**, *142*, 2250.
(6) Kato, M.; Yazawa, Y.; Okinaka, Y. *Int. Technol. Conf. Proc., Am. Electroplaters Surf. Finishers Soc.* **1995**, *813*, 805.
(7) Osaka, T.; Kodera, A.; Misato, T.; Honma, T.; Okinaka, Y. *J. Electrochem. Soc.* **1997**, *144*, 3642.
(8) Reid, F.; Goldie, W. *Gold Plating Technology*; Electrochem. Pub. Ltd.: Bristol, Great Britain, 1974.

10.1021/cm001051y CCC: $19.00
Published on Web 09/21/2000

ramic powders or nanophase diamond.

Low-density submicrometric and nanophase powders were preferred to the usual micrometric materials to achieve the following requirements: (i) to maintain high fineness; (ii) to maintain the bright yellow color typical of pure gold; and (iii) to disperse particles in the entire volume of the electrolytic bath homogeneously, with mechanical stirring alone.

As_2O_3 may be used to deposit gold films at high current density, yielding bright coatings.[1,15] As_2O_3 was therefore added to the electrolytic bath in order to study the concurrent effects of hardening additives and grain refiners.

Many aspects related to involved mechanisms and final product properties can be set, correlating the data obtained by means of various methodologies. In this investigation, information on film composition and morphology has been obtained by analyzing the deposits by means of secondary ion mass spectrometry (SIMS) and scanning electron microscopy (SEM). The potential of the SIMS technique for characterization of metals and metal oxide thin films has been well evidenced:[16,17] deposit components were identified, highlighting any eventual additives and impurities included during synthesis but not detectable by means of less sensitive analytical procedures. Furthermore, the distributions of major and minor components through the film were studied by analyzing related ion depth profiles. SEM analyses were carried out for information on deposit morphology modifications induced by powder inclusions and varying experimental conditions. By means of sample cross-sectional investigations, deposit thickness could be measured, giving an estimate of electrodeposition rates and SIMS sputtering rates. Therefore, SIMS and SEM were used widely in the present work, and the results regarding powder inclusions are reported here.

Finally, effects on deposit hardness due to powder addition were estimated by means of preliminary microhardness tests based on the Vickers scale.

Experimental Section

Bath compositions and working conditions for the studied codeposits are listed in Table 1. All chemicals were reagent-grade; H_2O used for the electrolyte solutions was Millipore-grade (Millipore Corp., Bedford, MA). The powders added to the electrolytic bath and their sizes are listed in Table 2. Cu sheets (1.0 × 1.0 cm^2; 0.1 cm thick) were used as cathodic substrates, degreased before electrolysis with trichlorethylene, etched with HCl, and carefully rinsed with water.[1] Electrolyses were carried out galvanostatically applying a constant current ranging from 1 to 2 mA cm^{-2} in a two-electrode single-compartment cell; a Pt coil facing the cathode was the counterelectrode (anode/cathode surface ratio ≃30). Current density and hydrodynamic conditions were defined according to the Guglielmi codeposition model.[19−21] Electrolyses were also carried out under mechanical stirring and an N_2 atmosphere, to inhibit the Au(I) dismutation reaction.[22]

Table 1. Composition and Working Conditions of Au Electrodeposition Bath

Au (III) as $HAuCl_4$	4 g L^{-1}
HCO_3^-/CO_3^{2-}	0.5 M
Na_2SO_3	0.17 M
EDTA	0.061 M
alkylamine	$3.9 \cdot 10^{-3}$ M
As_2O_3[a]	0.12 g L^{-1}
ceramic powders	0.83 g L^{-1}
diamond	0.033−0.1 g L^{-1}
pH	9
temperature	40 °C
j	1−2 mA cm^{-2}

[a] For those baths containing As_2O_3.

Table 2. Micrometric and Submicrometric Powders[a] Used as Hardening Agents

sample	powder	average grain size (μm)
A	SiC	0.23
B	SiC ultrafine	0.04
C	Si_3N_4	0.19
D	TiO_2	0.005
E	diamond[b]	0.005

[a] Powders furnished by CNR laboratories (IRTEC Faenza, TEMPE Milan) and CISE Milan. [b] Nanophase diamond obtained by explosive process.[18]

All electrochemical experiments were performed on a PAR model 263A potentiostat−galvanostat, controlled by software 273A EG&G PARC (EG&G Instruments, Princeton Applied Research, Princeton, NJ).

A custom-built instrument was used to carry out SIMS analyses. A monochromatic (6 keV) O_2^+ ion beam collimated to 50 μm was generated in a mass-filtered duoplasmatron ion gun (model DP50B, VG Fisons, U.K.). A powerful mass-energy analyzer (model EQS1000, Hiden, U.K.) with a high-transmission 45° sector field energy analyzer and a quadrupole mass-filter was used for negative- and positive-ion detection in counting mode. Lens and energy analyzer potentials, quadrupole electronic control units, and the detection system were controlled via a Hiden HAL IV interface. Because of the spectrometer resolution power (±1 *m*/*z* unit), the ion species were identified by resolving the overlapping *m*/*z* signals with an isotope pattern simulation program. In this way, the confidence interval and residual standard deviations could be calculated for detected ion groups to discriminate their various contributions. Therefore, by following signals of interest as a function of bombarding time, ion depth profiles were analyzed.

As mentioned in the Introduction, sputtering rate, estimated by cross-sectional SEM micrographs, was between 200 and 300 nm min^{-1}, depending on the size of the raster (ionic current range between 400 and 800 nA).

Scanning electron microscopy (Cambridge Stereoscan 440) together with energy-dispersion X-ray system (EDS) microanalysis (PV9800 Philips) was used to characterize surface deposit morphology.

Microhardness was measured with a Vickers hardness indenter (Leitz Wetzlar), applying a 50 g load to sample surfaces for 30 s; for each deposit, the average value (±10% deviation) was obtained with five measurements in different areas.

(9) Roos, J. R.; Celis, J. P.; Helsen, J. A. *Trans. 1nstitute Met. Finish.* **1977**, *55*, 113.
(10) Greco, V. P. *Plat. Surf. Finish.* **1989**, *76* (7), 62.
(11) Sadowska-Mazur, J.; Warwick, M. E.; Walker, R. *Trans. 1nstitute Met. Finish.* **1986**, *64* (4), 142.
(12) Hwang, B. J.; Hwang, C. S. *J. Electrochem. Soc.* **1993**, *140*, 979.
(13) Bozzini, B.; Cavallotti, P. L.; Giovannelli, G.; Brevaglieri, B.; Natali, S.; Signorelli, G. *Convegno Nazionale AIM − Atti del Convegno* **1997**, 875.
(14) Zielonska, R. *Gold Technol.* **1994**, *14*, 38.
(15) Piccirillo, C.; Buchberger, A.; Fabrizio, M.; Calliari, I.; Dabalà, M. *EMAS '99*, Konstanz, Germany, 3−7 May, 1999; p 328.
(16) Daolio, S.; Kristof, J.; Piccirillo, C.; Pagura, C.; De Battisti, A. *J. Mater. Chem.* **1996**, *6*, 567.
(17) Wilson, R. G., Stevie, F. A., Magee, C. W., Eds. *Secondary Ion Mass Spectrometry*; J. Wiley & Sons: New York, 1989.
(18) Bozzini, B.; Giovannelli, G.; Nobili, L.; Cavallotti, P. L. *A. I. F. M.* **1995**, *46*, 92.
(19) Guglielmi, N. *J. Electrochem. Soc.* **1972**, *119*, 1009.
(20) Celis, J. P.; Roos, J. R. *J. Electrochem. Soc.* **1977**, *124*, 1502.
(21) Narayan, R.; Nayarana, B. *Rev. Coatings Corros.* **1981**, *4*, 113.
(22) Socha, J.; Safarzynski, S.; Zak, T. *J. Less-Common Met.* **1975**, *43*, 283.

Results and Discussion

The electrolyses, carried out as Table 1 reports, gave bright and golden films. By the addition to the electrolytic bath of the powders listed in Table 2, these characteristics slightly changed; due to the increased composite roughness, and notwithstanding the coarse control of mechanical stirring and N_2 bubbling during the electrolyses, they were reproducible. Moreover, by the addition of As_2O_3 to the baths, the deposit surfaces became smoother and, as a consequence, brighter.

To select the most advantageous additives, the preliminary experiments were carried out by also testing Al_2O_3, B_4C, TiN, and TiB_2. The obtained results are not reported here, but their performances were promising enough, except for TiB_2. In fact, to avoid TiB_2 powder accumulation on cathode surface, it would have been necessary to add deflocculating compounds that gave very rough and mat deposits.

SIMS Analysis. Mass spectra were taken in both positive and negative ion modes, to determine surface composition and therefore additive inclusions in gold films. The main ion species related to the codeposits are listed in Table 3. Besides the species reported here, organics, water, and support peaks were evidenced, and in particular, several arsenic-related signals (i.e., AsO_x^+, $x = 0-1$; AsO_x^-, $x = 2-4$) were found on the spectra of coatings electrodeposited from the As-containing bath. In all codeposits, additive, Au, and Au−additive peaks were present, although Au−organic peaks were detected only on the blank sample surfaces. Furthermore, a careful comparison of blank and codeposit mass spectra illustrated many remarkable features.

The negative-ion mass spectrum of a blank sample (Figure 1a) showed some interesting data: S^-, Cl^-, and carbonaceous fragments (C_2^-, $CN^-/C_2H_2^-$, CNO^-, etc.) coming from the electrolyte were highlighted. $AuCNO_x^-$ and Cl-containing mixed clusters could also be detected, confirming the adsorption of organic species on the cathode surface during electrodeposition. AuO_x^- peaks ($x = 0-2$) were present, too; the $AuCuO^-$ signal ($m/z = 276$) was also detected and related to metal-substrate interdiffusion phenomena.[23] As will be seen in detail below, the relative intensities of these species are remarkably affected by matrix properties, due to powder inclusion.

Figure 1b shows the negative-ion mass spectrum for a gold film deposited from TiO_2-containing electrolyte: Ti-corresponding signals can be identified, showing the presence of TiO_2 powder on the surface. $AuTiO_x^-$ ($x = 2, 3$) peaks are also clear, suggesting interactions between gold and TiO_2 powder. Several differences with respect to the blank negative-ion spectrum were observed: by the addition of TiO_2 to the deposition bath, $AuCNO_x^-$ clusters disappeared and the S^- contribution decreased remarkably. Isotopic pattern analyses, in fact, showed that $m/z = 32$ peak intensity was due mainly to O_2^- ion; besides $m/z = 34$ peak became negligible. Changes in AuO_x^- ion species were also seen: AuO^- was not evidenced, and the Au^-/AuO_2^- intensity ratio decreased considerably, due to the increasing AuO_2^- peak. This difference in ion yield indicates that the Au−TiO_2 codeposit has characteristics different from those of pure gold film, as expected for different matrixes. Au−Cu mixed clusters were not detected, confirming that Cu diffusion takes place to a much smaller extent in the presence of included particles.[1,15]

SiC powder (0.04 μm grain size) added to the electrolyte yielded the negative-ion mass spectrum of Figure 1c, which shows several Si-related peaks and a C_2^- signal ($m/z = 24$) much more intense than that in the spectra of parts a and b of Figure 1. As already observed,[1] C_2^- may be representative of inorganic carbon in gold films, and this fact was confirmed in this experiment. Here too, the matrix effect is noticeable in Au-related signals: the Au^-/AuO_x^- ($x = 1, 2$) ratios changed remarkably in comparison with blank ones; in particular, an increase in the AuO_2^- peak was observed, although it was less enhanced than for the Au−TiO_2 system. It was also interesting to observe that, as shown in Figure 1b, no S^- or Au−(organics) were evidenced; it is important to stress that these features were common to all codeposits, whatever the powder used as additive.

Table 3. Most Important Ion Species Detected in Surface Mass Spectra of Au Codeposits

	TiO_2		SiC or Si_3N_4		diamond[a]
m/z[b]	⊕	⊖	⊕	⊖	⊖
28			Si		
40				SiC[d]	
44			SiO		
45			SiOH		
48	Ti				
56			Si_2		
60				SiO_2	
64	TiO	TiO			
68				Si_2C[d]	
70			Si_2N[c]		
72			Si_2O	Si_2O	
80	TiO_2	TiO_2		Si_2C_2[d]	
88			Si_2O_2		
96	Ti_2	TiO_3		Si_2C_2O[d]	
112	Ti_2O		Si_4[c]		
120				Si_2O_4	
128	Ti_2O_2				
136				Si_2O_5	
144	Ti_2O_3				
152				Si_2O_6	
167				$AsSiO_4$[e]	
180				Si_3O_6	
183				$AsSiO_5$[e]	
196				Si_3O_7	
199				$AsSiO_6$[e]	
221					AuC_2
225			AuSi		
227				$AsSi_2O_6$[e]	
237			AuSiC[d]	AuSiC[d]	
239				AuSiN[c]	
241			AuSiO	AuSiO	
243				$AsSi_2O_7$[e]	
245	AuTi				
249			$AuSiC_2$[d]		
253			$AuSi_2$		
257				$AuSiO_2$	
269			$AuSi_2O$		
273				$AuSiO_3$	
277		$AuTiO_2$		$Au(SiC)_2$[d]	
285			$AuSi_2O_2$		
289				$AuSiO_4$	
293		$AuTiO_3$			

[a] No peculiar ion species were detected in positive spectra of Au−diamond codeposits. [b] Mass numbers calculated for most abundant isotope for each element. [c] For Au−Si_3N_4 codeposits. [d] For Au−SiC codeposits. [e] For As_2O_3-containing baths.

(23) Rapson, W. S. *Gold Bull.* **1996**, *29*, 61.

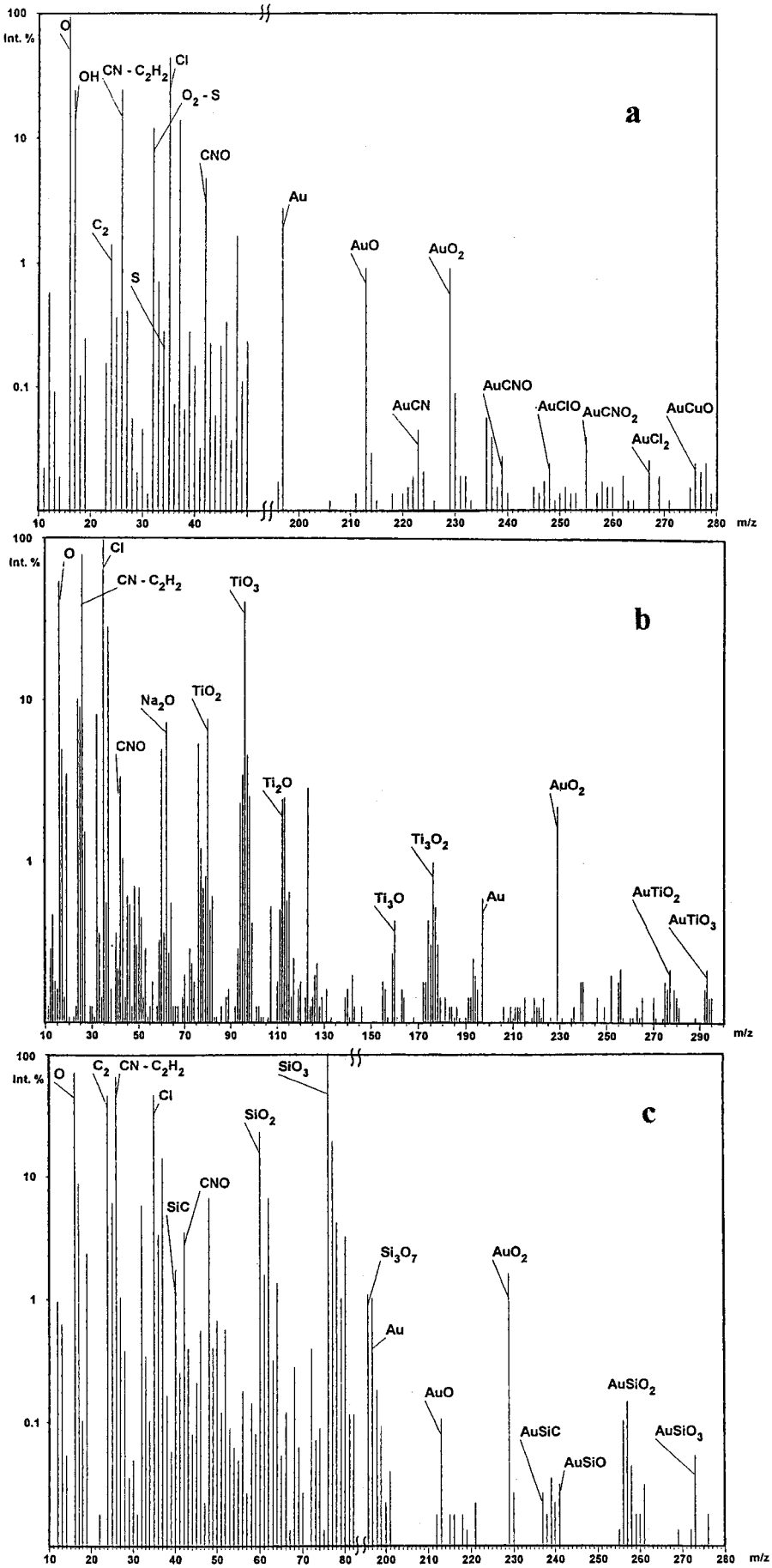

Figure 1. Negative-ion mass spectra: (a) Au blank sample, $j = 2$ mA cm^{-2}; (b) Au−TiO_2 codeposit, $j = 2$ mA cm^{-2}; and (c) Au−SiC codeposit, SiC average grain size = 0.04 μm, and $j = 1$ mA cm^{-2}.

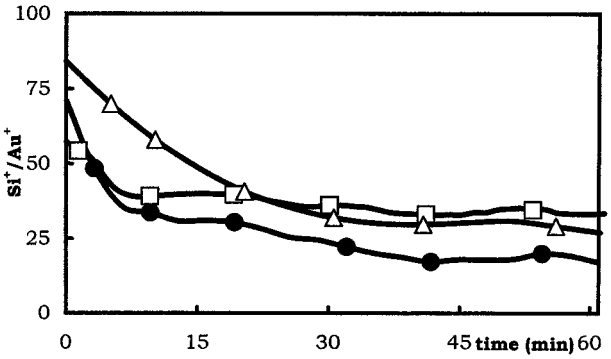

Figure 2. Si^+/Au^+ ion intensity ratio for Au−SiC codeposit: SiC average grain size = 0.04 μm and j = 2 mA cm^{-2}. Measurements were taken at three different points of the sample (●, △, □)

As regards the blank sample behavior, these ion fragments were clearly resolved in the mass spectrum (Figure 1a); their depth profiles showed first surface enrichment and then a constant shape in the inner regions at intensities comparable with those of the other Au clusters. The lack of S and Au−organic ion fragments in the spectra was thus attributed to inhibition of organic species and ligand adsorption caused by powder inclusion. The absence of Au−Cu signals was also a characteristic common to all codeposits, suggesting that support diffusion toward the film surface is limited by particle inclusion.

Several Au−Si mixed clusters were detected in the spectrum; compared with the Au−TiO_2 codeposit, more mixed ion species were found (see Table 3), indicating the high reactivity of silicon toward gold. Table 3 also shows that Au−Si_3N_4 codeposits behave similarly, suggesting that the high reactivity of silicon does not depend on the nature of ceramic powders.

Further evidence of Si reactivity was seen in the spectra of samples deposited from a Si_3N_4- and As_2O_3-containing bath (Table 3). Mixed clusters containing species from hardening and brightening agents (for instance, $AsSiO_x^-$) were in fact only observed in Si-based ceramics.

As regards Au-diamond films, sharp C_2^- signal increases were observed.[1] Nevertheless, in the lower mass range, peaks corresponding to organic fragments ($CH_x^{\pm}$, $x = 0-3$; $C_2H_x^-$, $x = 0-2$; CNO_x^-, $x = 0,1$) were slightly higher than those in the blanks, in both positive- and negative-ion modes. For higher m/z values, the AuC_2^- (m/z = 221) mixed cluster was also seen.

To study additive distribution through the films, the behavior of some signals was followed as a function of bombarding time. Figure 2 shows Si^+/Au^+ intensity ratios according to bombarding time for Au−SiC codeposits. Measurements were taken at three different points of the sample to establish distribution homogeneity: all three curves may be seen to decrease in the outer regions of the film and then become constant in the bulk, revealing ceramic enrichment in the surface layers.

In the case of a deposit obtained from a bath containing both Si_3N_4 and As_2O_3, the Si^+/Au^+ ratio behaved similarly to those of Figure 2. The AsO^+/Au^+ ratio (to analyze arsenic distribution, the AsO^+ signal was preferred to that of As^+, which showed a low ion yield) had flat behavior for the whole investigated depth, confirming the reduction of As(III) to As(0), with the formation of an intermetallic compound with constant stoichiometry.[24] These observations highlight the fact that both hardening and brightening additives also occur in the inner layers of the deposit. In these composites, a sharp increase in the Cu^+/Au^+ ratio after 15 min of bombardment revealed that the support material had been reached. Moreover, as already mentioned,[1] the absence of Cu surface accumulation suggests that its migration is inhibited, due to the inclusion of strong small particles in the Au film.[25]

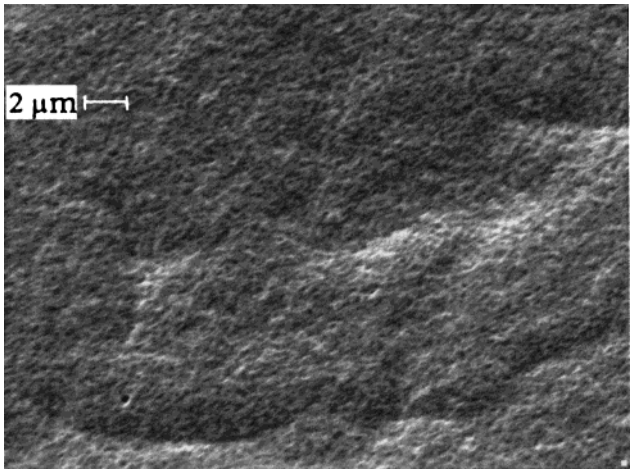

Figure 3. SEM micrograph of Au film (blank sample): j = 2 mA cm^{-2}.

As Table 2 shows, three different quantities of nanophase diamond were added to the electrodeposition bath. C_2^-/AuO_2^- ion intensity ratios were analyzed for samples deposited with different additive concentrations and, in one case, with As_2O_3 together with powder in the electrolyte. In all of the deposits, surface accumulation was followed by signal stabilization; therefore, it may be stated that, in comparison with that of gold, diamond distribution was not affected in the observed range by its concentration in solutions or by the presence of As_2O_3.

SEM Microstructure. The surface morphology of codeposits was investigated by SEM. Figure 3 shows a SEM photomicrograph of a blank sample: note how its surface is completely featureless, even at 4500×, like that of gold deposited from sulfite baths.[26]

Figure 4 shows to what extent the addition of nanometric diamond to the electrolyte affected deposit structure: the film deposited from a solution containing 0.1 g L^{-1} of powder appeared much more porous. The surface SEM micrograph (Figure 4a) revealed the presence of an oriented dendrite structure. Films deposited from a bath with lower diamond content had the same morphology, indicating that changes in powder concentration do not influence deposit structure. The sample cross section (Figure 4b) shows the columnar growth of the film and its roughness.

The addition of As_2O_3 to the diamond-containing electrolyte induced drastic changes in deposit structure. As shown in Figure 4c, the film appeared less porous, and its aspect was smooth and bright. Similar to obser-

(24) Dinan, T. E.; Cheh, H. Y. *J. Electrochem. Soc.* **1992**, *130*, 410.
(25) Higgins, R. A. *Engineering Metallurgy*; Edward Arnold; London 1993.
(26) Craig, S. E.; Harr, R. E.; Henry, J.; Turner, P. *J. Electrochem. Soc.* **1970**, *117*, 1450.

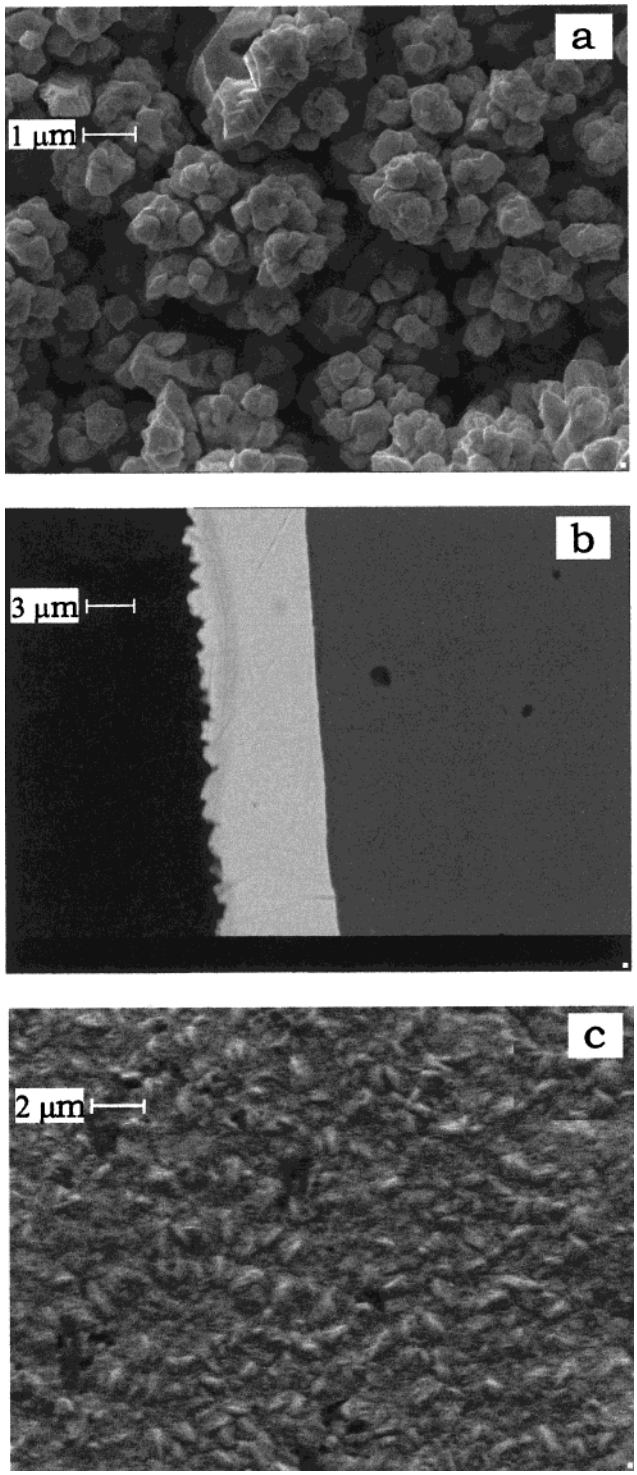

Figure 4. SEM micrographs of Au−diamond codeposit, with diamond 0.1 g L^{-1} and $j = 2$ mA cm^{-2}: (a) surface morphology; (b) deposit cross section; and (c) As_2O_3, 0.12 g L^{-1}.

vations made with various gold electrolytes,[24] arsenic clearly acted as a good grain refiner. In our case, arsenic was not detected by EDS analysis, indicating that its concentration was lower than the EDS detection limit (<0.1 wt %[27]). This is in agreement with the literature: [24] in similar experimental conditions, arsenic concentration in the deposits was estimated in the range 0.1−0.3 wt %.

(27) Pella, P. A. In *Instrumental Analysis*; Christian, G. D., O′Reilly, J. E., Eds.; Allyn and Bacon: Newton, Massachusetts, 1986.

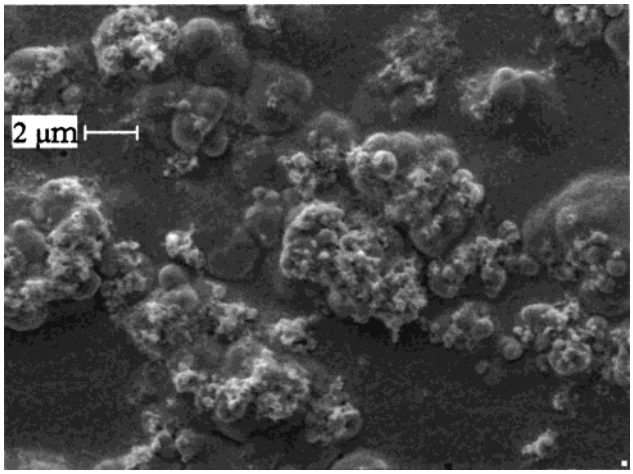

Figure 5. SEM micrograph of Au−SiC codeposit: SiC average grain size = 0.04 μm; $j = 2$ mA cm^{-2}.

SEM surface analysis showed the modifications in morphology induced by the nature of the powders, despite their chemical/electrochemical inertness. All of the codeposits, in fact, exhibited different morphology depending on the powder used. As an example, Figure 5 shows an Au−SiC codeposit (average granulometry = 0.04 μm), obtained at the same current density used for the Au-diamond codeposit in Figure 4a.

Powder granulometry was also considered an important parameter. To investigate its influence on deposit characteristics, SiC powder was used with two different grain sizes (Table 1); Figure 6 shows a SEM micrograph of a Au−SiC codeposit with average ceramic grain sizes of 0.23 and 0.04 μm, both deposited at 1 mA cm^{-2}. Differing morphologies were observed, and the grains of Figure 6a were smaller and closer than those of Figure 6b. Furthermore, higher granulometry corresponded to powder surface enrichment, detected by EDS. Some preliminary X-ray photoelectron spectroscopy (XPS) data[28] fit these results, and a more enhanced surface accumulation was shown for the larger SiC particles during sputtering.

The influence of current density may also be compared in the micrographs of Figures 5 and 6b: films were deposited using the same additive (SiC, 0.04 μm average grain size) but at different current densities (2 and 1 mA cm^{-2}, respectively). It was observed that the coating deposited at 1 mA cm^{-2} had a more regular structure than the corresponding one at 2 mA cm^{-2}; grain size was also smaller. However, as already noted with arsenic, no Si signals were detected by EDS for 0.04 μm SiC, even though they were evidenced by SIMS.

With the addition of As_2O_3 (see Figure 7), the effect was the same as that already observed for the Au−diamond codeposit: grain size decreased and the structure became much more regular, confirming the grain-refining properties of arsenic (Figure 7).

Hardness Tests. Preliminary microhardness tests were carried out: due to the thinness of the films (up to 10 μm), only a relative scale could be obtained, which displayed the influence of particle size on hardness. Figure 8 shows values measured for Au−SiC (both grain sizes), Au−TiO_2 (with/without As), and Au−diamond

(28) Unpublished results.

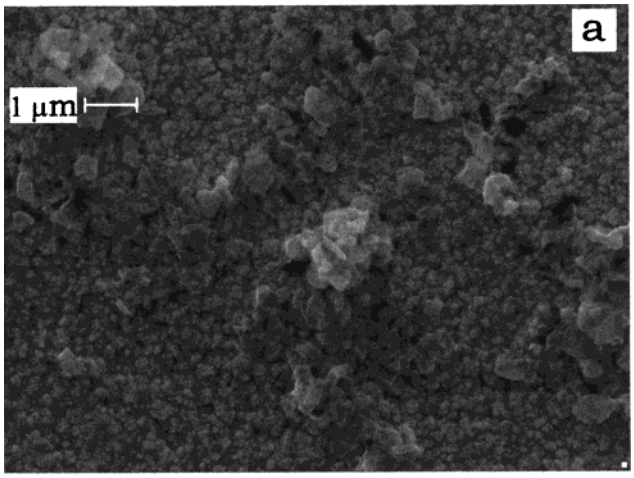

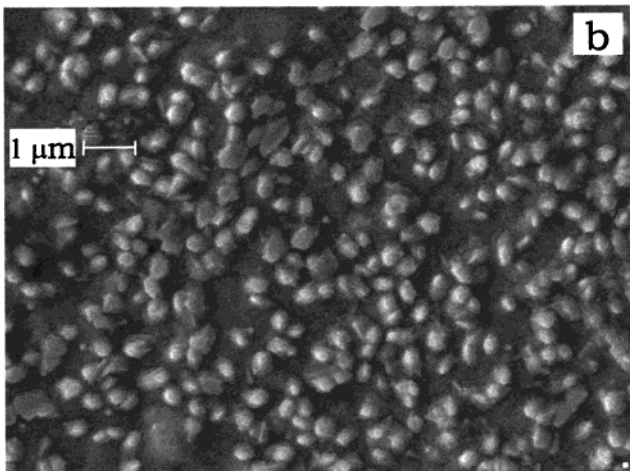

Figure 6. SEM micrographs of Au−SiC codeposits, with j = 1 mA cm^{-2}: (a) SiC average grain size = 0.23 μm, and (b) SiC average grain size = 0.04 μm.

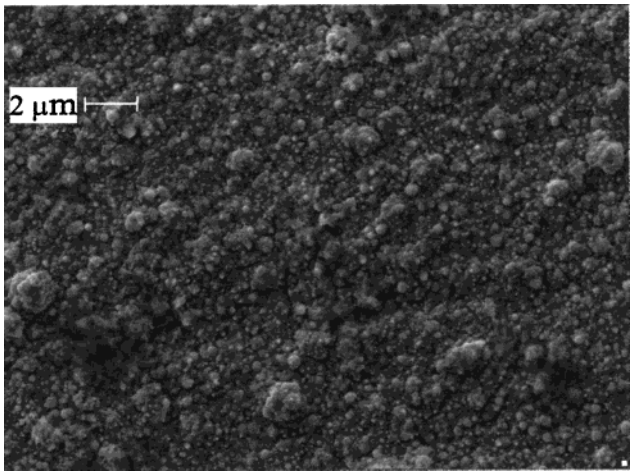

Figure 7. SEM micrograph of Au−SiC codeposits: As_2O_3, 0.12 g L^{-1}; SiC average grain size = 0.04 μm; j = 2 mA cm^{-2}.

codeposits. It can be seen that the SiC powder is effective as a hardening agent at 0.04 μm grain size, with its relative hardness value being higher than those for the Au−diamond codeposits. Instead, in the Au−TiO_2 sample, a slight decrease with respect to the blank was noted. Moreover, it is interesting to observe that the expected hardness increase for As-containing films was only seen for the deposit containing 0.23 μm SiC.

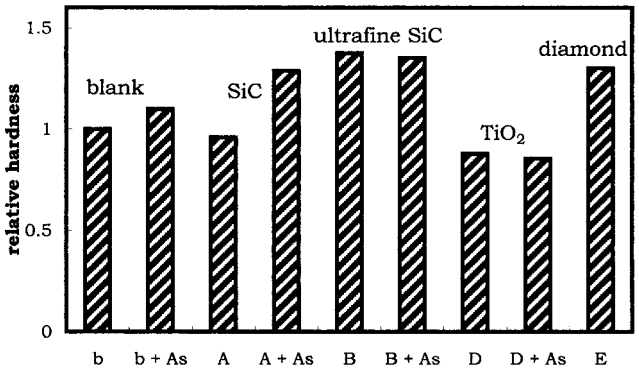

Figure 8. Relative hardness scale: (b) blank sample; (A) Au−SiC with 0.2 μm average grain size; (B) Au−SiC with 0.04 μm average grain size; (D) Au−TiO_2; (E) Au−diamond codeposits, with and without addition of As (j = 2 mA cm^{-2}).

Conclusions

Several Au composites were electrodeposited exploiting the inclusion of submicrometric and nanophase inert powders. This process was tested as a possible route for achieving Au films with suitable hardness characteristics and without any appreciable lowering of fineness in comparison with no-additive deposits.

The SIMS technique was helpful in studying surface and near-surface layers and deeper regions. Embedding of ceramic powders for the whole film depth was shown for all powders, with homogeneous distribution in all samples. The presence of arsenic as a brightening agent, added together with the ceramics, was also detected in all thin films. Electron microscopy techniques (SEM−EDS) gave information on how experimental conditions influence deposit structure: it was seen that the nature of the powders (despite their chemical inertness), the grain size, the presence of arsenic, and current density all affect deposit morphology.

Although the structural modifications induced by the additives were evident in all samples, only with the SIMS technique could all of the chemical species (powders and As) be detected. Considering the great sensitivity of SIMS, these results support the initial hypothesis that concentrations of submicrometric particles in deposits may be kept low with only slight decreases in gold fineness.

Due to the thinness of the Au deposits, a relative hardness scale was established, and the effects on the hardness were confirmed. In particular, of the powders in question, ultrafine SiC showed the best properties. To measure hardness for all additives, micro-indenting tests are indicated. Finally, mechanical tests will be carried out in order to establish improvements in workability and wear resistance.

Acknowledgment. We thank Dr. A. Bellosi (IRTEC-CNR, Faenza), Dr. E. Olzi (TEMPE-CNR, Milan), and Dr. M. Musci (CISE, Milan) for providing the ceramic powders and nanophase diamond used in the experiments and Ms. G. Walton for revision of the English text. This research was partially supported by "Pro.Art. Programma a sostegno della produzione e del commercio dell'Artigianato Orafo" of CNR and MICA, Rome, Italy, and by PF MSTA II of CNR, Rome, Italy.

CM001051Y